

Open-loop Combustion Timing Control of a Spark-Ignited Engine

Mathieu HILLION, Jonathan CHAUVIN, and Nicolas PETIT

Abstract—In this paper, we propose a control strategy to improve the combustion efficiency of Spark Ignited engines. More precisely, we adapt the spark ignition time according to variations of thermodynamic conditions of the combustion chamber during transients. Sensitivity of a simple proposed combustion model (ordinary differential equations governing the flame propagation phenomenon) is used to compute an open-loop control law. An end-point matching condition is formulated to guarantee that the middle of combustion occurs at an optimal time. Simulation results stress the relevance of the approach.

INTRODUCTION

The control technology found on most Spark Ignited (SI) automotive engines consists of an airpath controller, a fuelpath controller, and an ignitionpath controller. These subsystems collaborate to satisfy high-level orders from the driver (e.g. torque requests). The airpath subsystem primary objective is to control the air mass aspirated into the cylinders. Interestingly, usually no particular effort is made to control the other thermodynamic in-cylinder variables which are the temperature, the pressure, and the aspirated burnt gases mass. Fortunately, these variables eventually converge to values corresponding to the tracked aspirated air mass setpoint (and current engine speed). Yet, convergence can take time, because the airpath subsystem is repeatedly relatively slow.

During the frequent transients observed onboard vehicles, the pressure, temperature and aspirated burnt gases mass found in the cylinder at the beginning of the combustion are thus slightly different from optimally designed steady-state values. The values of the considered parameters depend on corresponding values at the intake valve closing (*ivc*). Several other disturbances also play a role, such as (VVT) actuation which can increase the mismatches. These VVT disturbances and the mentioned offsets at *ivc* have an important common property: they are measured, or can be accurately estimated. In this paper, we propose a method to compensate them. We now sketch it.

In theory, the ignitionpath controller handles the spark timing so that the middle of combustion (CA_{50} : Crankshaft Angle where 50% of the fuel has burned) occurs at an optimal instant. This guarantees a good combustion efficiency. Usual ignitionpath controllers compute the spark

timing based on static look-up tables accounting for the current working point. This approach assumes that the engine has reached some steady-state conditions. This is obviously wrong during transients when the thermodynamic parameters mismatch at the beginning of the combustion creates an offset (lead or lag) in the middle of combustion timing. Physically, the spark ignition time (*sit*) has a major synchronization effect on the whole combustion timeline. Theoretically, it is thus possible to use it to reach an ideal CA_{50} despite the discussed offsets in the thermodynamical parameters.

To compute the relevant updates in *sit*, we formulate a target reaching problem for a set of two non-linear differential equations over a variable time interval which depends on the *sit*. Equivalently, after a time change, this problem is turned into a shooting problem. At first order, a sensitivity analysis provides an explicit solution. After some inverse change of variables, an explicit procedure is obtained to determine the update in the *sit* to compensate the discussed offsets. In this very preliminary work, we wish to prove the concept that a phenomenological model can be exploited to complement static look-up tables during transients. Interestingly, this approach *does not require any in-cylinder sensor*. This point is supported by numerical results obtained with the AMESim Simulation software. Further work will include experimental validation.

The paper is organized as follows. Section I presents the motivations for the considered problem. In Section II we expose the main phenomena considered in our flame propagation model for SI engines along with some simplifying assumptions. In Section III, we formulate a control problem which is solved in Section IV. In Section V, we provide numerical results. Finally, in Section VI, we propose future developments and explain how our proposed technique can be embedded into existing SI engine control systems.

I. MOTIVATIONS

In the context of environmental restrictions and sustainable development, pollution standards have steadily become more stringent over the last 20 years. In turn, engine pollutant emission reduction has become a topic of major interest for engine manufacturers. For that purpose, there is a general consensus that the combustion should be closely controlled. In theory, conventional (SI) engines produce low pollutant emissions levels. For sake of fuel consumption reduction, downsizing technologies (reduction of the engine size) and turbocharging have been developed and used along with Variable Valve Timing (VVT) devices (see [1]). A typical SI engine equipped with a turbocharger and VVT is depicted in Figure 1. VVT devices permit an internal Exhaust Gas

M. Hillion (corresponding author) is a PhD Candidate in Mathematics and Control, Centre Automatique et Systèmes, Mines ParisTech, 60, bd St Michel, 75272 Paris, France.

Email: mathieu.hillion@mines-paristech.fr

J. Chauvin is with the Department of Engine Control in Institut Français du Pétrole, 1 & 4 Avenue de Bois Préau, 92852 Rueil Malmaison, France.

N. Petit is with the Centre Automatique et Systèmes, Mines ParisTech, 60, bd St Michel, 75272 Paris, France.

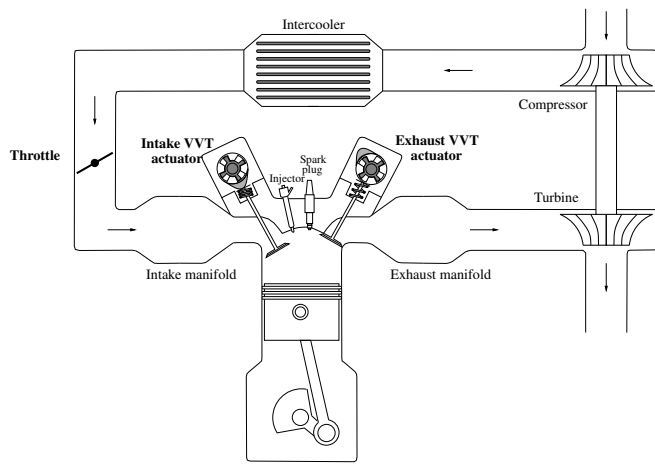


Fig. 1. Scheme of a Spark Ignited engine with VVT and Turbocharger.

Recirculation (iEGR) which reduces consumption and have significant beneficial effects in terms of Nitrogen Oxides (NO_x) emissions (see [2]).

SI engines use the combustion of a mixture of fresh air, burned gases, and fuel. The engine cycle takes place in three main phases pictured in Figure 2. These correspond to the airpath subsystem (which consists of the turbocharger, the throttle and the VVT actuators), the fuelpath subsystem (which consists of the injectors), and the ignitionpath (which consists of the spark plug). The air and burned gases cylinder filling task is carried out by the airpath subsystem. The fuel injection is achieved by the fuelpath subsystem, and the combustion is initiated by the ignitionpath subsystem. The

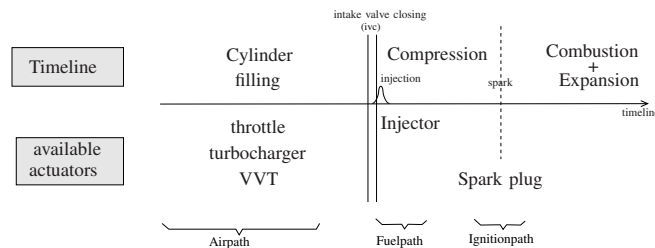


Fig. 2. Scheme of a Spark Ignited engine with VVT and Turbocharger.

TABLE I
ACRONYMS

SI	Spark Ignition
EGR	Exhaust Gas Recirculation
iEGR	internal Exhaust Gas Recirculation
BGR	Burned Gas Rate
<i>ivc</i>	Intake Valve Closing
<i>sit</i>	Combustion Ignition time (spark)
TDC	Top Dead Center
VVT	Variable Valve Timing
AFR	Air-to-Fuel ratio
NO_x	Nitrogen oxides
CA_{50}	Crankshaft angle where 50% of the Mass Fuel has Burnt

engine control system manages them all to guarantee that the engine produces a desired torque. We briefly detail these subsystems

A. Airpath control

Numerous airpath controllers have been designed (see [3]–[5]). Typically, they turn the driver’s torque demands into an in-cylinder air mass setpoint. In closed-loop, the airpath controller tracks the aspirated air mass setpoint. The considered actuators are the throttle, the turbocharger, and the VVT devices.

B. Fuelpath control

The fuelpath controller regulates the fuel injection. To maximize the efficiency of exhaust gases after-treatment devices, the Air to Fuel Ratio (AFR) has to be maintained as close as possible to the stoichiometric value (AFR_s) (see [6], [7]). Accordingly, the injected fuel mass is directly computed from the (estimated) value of the in-cylinder air mass m_{air} ($m_{inj} = \frac{1}{\text{AFR}_s} m_{air}$).

To make the mixture as homogeneous as possible, injection usually takes place during the intake phase. Then, fuel vaporization and mixing with air and burned gases are both completed when combustion starts.

C. Classical Ignitionpath control (engines without VVT)

The torque production level does not exclusively depend on the amount of injected fuel and air mass. Spark timing, which initiates the combustion, plays a great role in the quality of the combustion (efficiency and pollutant formation). A “global” criterion commonly used to evaluate the quality of the combustion is the CA_{50} . The role of the Ignitionpath controllers is thus to make the CA_{50} track an optimum value $\overline{\text{CA}}_{50}$ by adjusting the *sit*.

Because of the complexity of the combustion phenomenon, and in particular of the flame propagation, usual spark timing controllers are based on static look-up tables depending on the main parameters impacting the flame propagation. These are the engine speed N_e and the aspirated air mass m_{air} (provided by the fuelpath estimator). Other parameters such as pressure or temperature of the in-cylinder gases are assumed to be close to their steady-state value corresponding to the operating point (N_e, m_{air}).

D. Proposed Ignitionpath controller improvements

During transients, the airpath controller makes no particular effort to have in-cylinder thermodynamic variables (temperature, pressure, amount of burned gases) closely track their steady-state values. There exist temporary mismatches which, in fact, negatively impact on the combustion efficiency. Mainly, the culprit is the ignitionpath controller which ignores these mismatches, and simply applies an open-loop control value based on look-up table assuming in-cylinder thermodynamic variable have already reached their expected steady-state values.

This issue is worsened on VVT equipped engine. Indeed, the VVT actuators play an important disturbing role¹. The VVT actuators shift the valve lift to create iEGR which dilutes the air charge (and thus slows down the flame propagation (see [8])). Besides these beneficial effects, shifting the valve lift has also an impact on the turbulence in the chamber. The flame propagation, which depends on this turbulence, is then either accelerated or slowed down.

During transients, the effects of burned gases, pressure, temperature, and VVT disturbance on the flame propagation are significant. One can expect to improve the quality of the combustion (in terms of consumption) by alleviating the offsets of in-cylinder thermodynamic and physical (VVT positions) parameters. This can be done by updating the available *sit* look-up tables. Certainly, it would be convenient to build up new tables having four parameters (pressure, temperature, burned gases mass, and VVT position) as additional input values. Yet, this is totally unrealistic, because the required experimental workload would be gigantic.

Rather, in-cylinder sensors could be used to complement the static look-up tables. In [9], Eriksson *et al.* present a spark timing feedback control based on in-cylinder ion current sensor. Such solutions provide accurate control of the combustion efficiency but the use of high frequency in-cylinder sensor is costly and can be troublesome.

Therefore, we present a solution *requiring only sensors available on all commercial-line engines*. We propose to keep the available look-up tables having in-cylinder air mass and engine speed as input and to compute “dynamical corrections” of the *sit* to account for the discussed offsets. As will appear, the main advantage of the proposed method is that it computes corrections based on thermodynamic and physical parameters. These can easily be measured on most classical SI engines.

Corrective terms are computed based on a flame propagation model presented in the next section.

II. COMBUSTION MODELLING

We consider the propagation flame model presented in [10], which has been experimentally validated even during transients. It represents the cylinder volume as two zones (the burned zone and the unburned zone) separated by the flame which is modelled as a thin layer. During the whole combustion, the flame propagates from the burned zone towards the unburned one. The model relies on the following assumptions

- homogeneity of the mixture and pressure equilibrium between the two zones;
- perfect mixing of the three gases: air, burned gases and fuel vapor;
- stoichiometric combustion;
- no spatial dependencies of the different variables.

The main elements appearing in the model are

¹Additionally, the VVT actuators can also be used to speed up the airpath dynamics, which in turn, introduces further offsets from the expected steady-state.

- the combustion kinetics;
- the laminar burning speed of the flame front;
- the flame front geometry;
- the turbulent kinetic energy (due to tumbling);
- the turbulence wrinkling of the geometrical surface;
- the wall heating losses.

Further, we choose to neglect the wall heating losses of the model. Table II gathers notations used throughout the paper.

TABLE II
NOMENCLATURE

Symb.	quantity	Unit
N_e	engine speed	rpm
θ	crankshaft angle	[deg]
θ_{ivc}	<i>ivc</i> crankshaft angle	[deg]
θ_{TDC}	top dead center crankshaft angle	[deg]
θ_{sit}	<i>sit</i> crankshaft angle	[deg]
$V(\theta)$	cylinder volume	m ³
V_{ivc}	cylinder volume at <i>ivc</i>	m ³
$P(\theta)$	in cylinder pressure	Pa
P_{ivc}	in cylinder pressure at <i>ivc</i>	Pa
$T(\theta)$	in cylinder temperature	K
T_{ivc}	in cylinder temperature at <i>ivc</i>	K
$T_u(\theta)$	unburned zone temperature	K
AFR_s	stoichiometric air/fuel ratio	-
m_{air}	aspirated air mass	kg
m_{bg}	in cylinder burned gases mass	kg
M_f	injected fuel mass	kg
m_f	mass of fuel burned (ranges from 0 to M_f)	kg
ρ_u	unburned zone density	kg/m ³
$(\rho_u)_{ivc}$	unburned zone density at the <i>ivc</i>	kg/m ³
Y_u	unburned zone fuel mass fraction	-
U	laminar burning speed	m/s
Ξ	turbulent wrinkling	-
γ	ratio of specific heats	-
Q_{LHV}	low heating value	J/kg
A	piston head surface	m ²
S_{fl}	flame surface area	m ²
S_{geo}	geometric flame surface area (without wrinkling)	m ²
f_{vol}	minimal flame volume (initiation of the flame)	m ³
x	mass fraction of burned fuel	-
y	$P.V^\gamma$	Pa m ^{3γ}

A. Fraction of burned mass of fuel x

The dynamics of the fraction of burned mass of the fuel x is given by (1) (see [10])

$$\frac{dx}{dt} = \frac{1}{M_f} \cdot \rho_u \cdot Y_u \cdot U \cdot S_{fl} \quad (1)$$

where M_f is the injected fuel mass, ρ_u is the mean density of the unburned gases, Y_u is the fuel mass fraction in the unburned zone, U is the laminar burning speed, and S_{fl} is the flame surface.

Because of the homogeneity assumption, Y_u is constant. We assume that the unburned zone is compressed by the

expansion of the flame. Neglecting the wall heating losses, and the heat exchange between burned gases and unburned gases leads to consider an isentropic compression of the unburned gases (we note the isentropic parameter γ). Then, the density can be inferred from the pressure using the isentropic relation $\rho_u/P^{1/\gamma} = cst$ and the thermodynamic conditions at *ivc*:

$$\rho_u = (\rho_u)_{ivc} \left(\frac{P}{P_{ivc}} \right)^{1/\gamma}$$

B. Laminar burning speed U

The correlation of Metghalchi and Keck expresses the laminar burning speed of a flame propagating in a mixture of fresh-air burned-gases and fuel (see [8], [11])

$$U = U_0 \left(\frac{T_u}{T_{amb}} \right)^\alpha \left(\frac{P}{P_{amb}} \right)^\beta \left(1 - 2.1 \frac{m_{bg}}{m_{bg} + m_{air}} \right) \quad (2)$$

where U_0 , α and β are constant parameters depending on the AFR, T_u is the temperature of the unburned gases, P is the pressure in the combustion chamber, and P_{amb} and T_{amb} are constant parameters. Following the assumptions of Section II-A, we compute T_u from the current pressure P using the isentropic relation and thermodynamic conditions at *ivc*

$$T_u = T_{ivc} \left(\frac{P}{P_{ivc}} \right)^{(\gamma-1)/\gamma}$$

C. Flamme surface S_{fl}

Following [8], [10], the flame surface is defined as

$$S_{fl} = S_{geo} \cdot \Xi \cdot f_{wall} \quad (3)$$

where S_{geo} is the geometric surface of the flame, Ξ represents the surface wrinkling, and f_{wall} is the wall destruction term.

1) *Geometric surface S_{geo}* : The geometric surface is a macroscopic measure of the flame surface which neglects the wrinkling phenomenon. In this paper, we use a geometric shape of the flame surface which is different from the one presented in [10]. Rather, we assume the following:

- at the beginning of the combustion, the flame has a spherical shape;
- when its diameter equals the distance from the piston to the cylinder-head (defined as V/A where A is the cylinder-head area), the flame becomes a truncated sphere from which 2 spherical caps are cut-off (see figure 3).

Analytically, the geometric surface is defined as a function of the flame volume V_{fl} as

$$S_{geo}(V_{fl}, \theta) = \begin{cases} \sqrt[3]{36\pi} \cdot V_{fl}^{2/3} & \text{if } V_{fl} < \frac{\pi}{6} \left(\frac{V(\theta)}{A} \right)^3 \\ 2\sqrt{2\pi V_{fl} \frac{V(\theta)}{A} + \frac{4}{3}\pi^2 \left(\frac{V(\theta)}{A} \right)^4} & \text{if } V_{fl} > \frac{\pi}{6} \left(\frac{V(\theta)}{A} \right)^3 \end{cases} \quad (4)$$

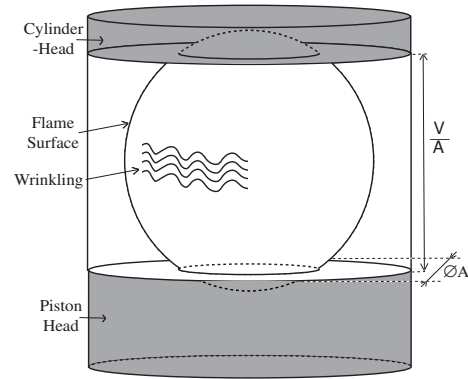


Fig. 3. Flame shape during propagation. Eventually, two caps are cut-off from the spherical surface.

The flame volume V_{fl} can be easily computed from the mass fraction of fuel burned x and the in-cylinder pressure, considering homogeneity of the mixture. To model the spark initiation of the flame, this value is only considered if the flame volume has reached a minimal value f_{vol} ; if not, the flame volume value is set to f_{vol} .

2) *Wrinkling Ξ* : The wrinkling of the flame surface is due to the turbulent kinetic energy. It increases the actual flame surface. At the beginning of the combustion, the flame is too small to be wrinkled, Ξ is then equal to one. As the flame gets wider, Ξ increases, meaning that the flame is wrinkled by the turbulent kinetic energy k . A typical model for Ξ is (see [10])

$$\Xi = 1 + \text{sigm}(V_{fl}) \frac{\sqrt{k}}{U} \quad (5)$$

where *sigm* is a scaled sigmoid function (e.g. tanh). The turbulent kinetic energy k mainly arises from the tumbling phenomenon observed in the chamber (swirl motion, spray injection and squish effects can be neglected [10]). The variations of k are modeled by a first order differential driven by the tumbling energy. Formally, we have

$$\frac{dk}{d\theta} = -\frac{C_{turb}}{m_{air} + m_{bg}} \frac{dE_{kin}}{d\theta} - C_{diss}k(\theta) \quad (6)$$

where C_{turb} and C_{diss} are constant positive parameters. E_{kin} is the kinetic energy associated to the tumbling which can be computed (see [10]) assuming the tumbling is a simple cylindrical rotation around the longitudinal axis of the total mass of gases in the cylinder volume. Equation (6) is analytically solvable from the *ivc* initial conditions. Therefore, it is not considered as a state equation.

3) *Wall destruction term f_{wall}* : The wall destruction term f_{wall} accounts for the reduction of the flame surface when it reaches the chamber walls. f_{wall} is then close to 1 during the first part of the combustion, dropping smoothly to 0 when the flame approaches the walls. In our control approach, we aim at controlling the CA₅₀. The model is not used after the CA₅₀. Thus, the simplifying assumption that the wall destruction term is 1 from the *ivc* to the CA₅₀ can be considered at no expense.

$$\left\{ \begin{array}{l}
\frac{dx}{d\theta} = \frac{1}{N_e} \left(\frac{C_1 \cdot p_2}{V(t)^{\kappa\gamma+1}} \cdot y^{\kappa+1/\gamma} + \frac{C_2 p_1^{-1/\gamma} \sqrt{k(\theta, p_3)}}{V(t)} y^{1/\gamma} \tanh \left(\frac{1}{r_0} \left(\frac{3V_{fl}}{4\pi} \right)^{1/3} - 1 \right) \right) S_{geo}(V_{fl}, t) \\
V_{fl} = \max(f_{vol}, V(\theta)(1 - (1-x)p_1^{1/\gamma}y^{-1/\gamma})) \\
S_{geo}(V_{fl}, \theta) = \begin{cases} \sqrt[3]{36\pi} \cdot V_{fl}^{2/3} & \text{if } V_{fl} < \frac{\pi}{6} \left(\frac{V(\theta)}{A} \right)^3 \\ 2\sqrt{2\pi V_{fl} \frac{V(\theta)}{A} + \frac{4}{3}\pi^2 \left(\frac{V(\theta)}{A} \right)^4} & \text{if } V_{fl} > \frac{\pi}{6} \left(\frac{V(\theta)}{A} \right)^3 \end{cases} \\
k(\theta, p_3) = C_3 \left(- \int_{p_3}^{\theta} \zeta'(z, p_3) e^{\frac{C_4}{N_e}(z-p_3)} dz + C_5 \right) e^{-\frac{C_4}{N_e}(\theta-p_3)} \\
\zeta(\theta, p_3) = V(\theta)^2 \left(\frac{\theta - \theta_{TDC}}{p_3 - \theta_{TDC}} \right)^2 \delta_{\theta < \theta_{TDC}} \\
\frac{dy}{d\theta} = Q_{LHV} M_f (\gamma - 1) V(\theta)^{\gamma-1} \frac{dx}{d\theta} \\
x(\theta_{sit}) = 0 \\
y(\theta_{sit}) = p_1
\end{array} \right. \quad (8)$$

D. Flamme propagation model

Once gathered, Equations (1), (2), (3), (4), (5), and (6) under its integral form allow to express the evolution of the flame propagation using two main variables: the burned fuel mass fraction x , and the in-cylinder pressure P . Equation (1) is a first state equation. A second one can be obtained from the classic relation between the fuel heat release and the pressure rise (see [8]), when wall heat losses are neglected

$$\frac{1}{(\gamma - 1)V^{\gamma-1}} \frac{d(PV^\gamma)}{d\theta} = Q_{LHV} M_f \frac{dx}{d\theta} \quad (7)$$

Eventually, (1)-(7) are a set of two states equations for the flame propagation (see System (8)). One state is the burned fuel mass fraction (x) and one state represents the pressure ($y \triangleq PV^\gamma$). In (8), five known constant parameters $\{C_i | i = 1..5\}$ appear. Additionally, three varying parameters p_1 , p_2 , and p_3 also come into play. They account for the offsets of the thermodynamical variables (pressure, temperature and burned gases mass) and physical parameters (VVT positions) discussed in Section I-D. Namely, they are

$$\begin{aligned}
p_1 &= P_{ivc} V_{ivc}^\gamma \\
p_2 &= \left(\frac{T_{ivc}}{P_{ivc}^{\frac{\gamma-1}{\gamma}}} \right)^\alpha \frac{(1 - 2.1 \frac{m_{bg}}{m_{bg} + m_{air}})}{P_{ivc}^{1/\gamma} V_{ivc}} \\
p_3 &= \theta_{ivc}
\end{aligned}$$

All these three parameters can be computed using measured or estimated signals. In details,

- θ_{ivc} is the *ivc* crankshaft angle. It is solely dependent on the VVT actuators positions which are usually measured with good accuracy. Interestingly, the influence of the turbulence on the combustion comes only into play by the *ivc* timing θ_{ivc} ;
- V_{ivc} is the cylinder volume at *ivc*. It is known very accurately;
- P_{ivc} is equal to the measured intake manifold pressure at the *ivc*. This statement relies on the assumption that

a pressure equilibrium is reached at the *ivc* between cylinder and intake manifold;

- m_{air} and m_{bg} can be obtained using an appropriate cylinder filling model (see [12], [13]);
- T_{ivc} can be computed using the measured fresh air temperature and a burned gases temperature model.

III. CONTROL PROBLEM

Formally, the flame propagation model (8) has the following general structure

$$\left\{ \begin{array}{l}
\frac{dx}{d\theta} = f(x, y, p, \theta) \\
\frac{dy}{d\theta} = g(x, y, p, \theta) \\
x(\theta_{sit}) = 0 \\
y(\theta_{sit}) = C^T \cdot p \\
\theta \in [\theta_{sit}, CA_{50}]
\end{array} \right. \quad (9)$$

where x is the fuel mass fraction burned (ranging from 0 to 1), y is an image of the in-cylinder pressure ($y \triangleq PV^\gamma$), θ is the crankshaft angle, and $p \triangleq (p_1, p_2, p_3)^T$ are the parameters to compensate using θ_{sit} . At steady-state, we assume that the airpath and VVT controllers have stabilized the parameters p to their reference value \bar{p} . Thus, a *reference combustion* takes place. It is the solution of

$$\left\{ \begin{array}{l}
\frac{d\bar{x}}{d\theta} = f(\bar{x}, \bar{y}, \bar{p}, \theta) \\
\frac{d\bar{y}}{d\theta} = g(\bar{x}, \bar{y}, \bar{p}, \theta) \\
\bar{x}(\bar{\theta}_{sit}) = 0 \\
\bar{y}(\bar{\theta}_{sit}) = C^T \cdot \bar{p} \\
\theta \in [\bar{\theta}_{sit}, \overline{CA}_{50}]
\end{array} \right. \quad (10)$$

This reference combustion defines a reference \overline{CA}_{50} (i.e. $\bar{x}(\overline{CA}_{50}) = \frac{1}{2}$). During transients, the parameters p are not

at their (steady-state) reference value \bar{p} which corresponds to the current working point (N_e, m_{air}) . We note

$$\delta p \triangleq p - \bar{p}$$

Thus, the transient combustion is temporarily different from the reference combustion, and the CA_{50} is not equal to its reference (i.e. $x(\overline{CA}_{50}) \neq \frac{1}{2}$).

We desire to control the CA_{50} to its reference value \overline{CA}_{50} by adding to the spark timing $\bar{\theta}_{sit}$ a correction $\delta\theta_{sit}$ counterbalancing the known disturbances δp . Formally, this is summarized under the following form

Problem 1. Consider the reference *sit* $\bar{\theta}_{sit}$ corresponding to the reference combustion (defined by (10)). It is desired to compute a *sit* correction $\delta\theta_{sit}$ such that the following system

$$\begin{cases} \frac{dx}{d\theta} = f(x, y, \bar{p} + \delta p, \theta) \\ \frac{dy}{d\theta} = g(x, y, \bar{p} + \delta p, \theta) \\ x(\bar{\theta}_{sit} + \delta\theta_{sit}) = 0 \\ y(\bar{\theta}_{sit} + \delta\theta_{sit}) = C^T \cdot (\bar{p} + \delta p) \\ \theta \in [\bar{\theta}_{sit} + \delta\theta_{sit}, \overline{CA}_{50}] \end{cases}$$

satisfies $x(\overline{CA}_{50}) = \frac{1}{2}$.

IV. SPARK TIMING CORRECTION COMPUTATION

We address Problem 1. The nonlinear nature of the differential equations to be solved (see (8)) makes the problem untractable by analytic methods. Thus, we propose to look for a first order solution obtained through a sensitivity analysis. For this purpose, the set of ordinary differential equations (9) is differentiated around the reference combustion defined as the solution for the following optimal parameters $(\bar{p}, \bar{\theta}_{sit})$. It is assumed that the following variables are known:

- \bar{p} , the reference parameters values;
- δp , the error between the actual and the reference parameters values;
- $\bar{\theta}_{sit}$, the reference *sit* value;
- \bar{x} and \bar{y} , the reference state corresponding to the reference combustion, which can be obtained by forward integration of (9).

A. Normalization of the time variable ($\theta \mapsto \tau$)

First, the following change of time is considered $T = CA_{50} - \theta_{sit}$ and $\theta = CA_{50} + (\tau - 1)T$. This yields a new system of equations

$$\begin{cases} \frac{dx}{d\tau} = F(x, y, p, \tau, T) \\ \frac{dy}{d\tau} = G(x, y, p, \tau, T) \\ x(0) = 0 \\ y(0) = C^T \cdot p \\ \tau \in [0, 1] \end{cases} \quad (11)$$

Similarly, for reference combustion values \overline{CA}_{50} , $\bar{\theta}_{sit}$, the change of time $\bar{T} = CA_{50} - \bar{\theta}_{sit}$, $\theta = \overline{CA}_{50} + (\tau - 1)\bar{T}$ yields the new formulation of the control problem

Problem 2. Consider a known value δp , find δT such that the system

$$\begin{cases} \frac{dx}{d\tau} = F(x, y, \bar{p} + \delta p, \tau, \bar{T} + \delta T) \\ \frac{dy}{d\tau} = G(x, y, \bar{p} + \delta p, \tau, \bar{T} + \delta T) \\ x(0) = 0 \\ y(0) = C^T \cdot (\bar{p} + \delta p) \\ \tau \in [0, 1] \end{cases}$$

reaches the target point $x(1) = \frac{1}{2}$.

B. Sensivity analysis

We propose to find an approximate solution at first order to Problem 2. One can easily verify that the considered system has a continuous and piecewise C^1 right hand side. We consider a natural extension of the classical result of Hale (see thm 3.3 of [14]) on the continuous dependency of a differential equation w.r.t initial conditions to piecewise C^1 right hand sides. The application mapping the parameter p to the solution z_p of the differential equation

$$\begin{cases} z'(t) = f(z(t), p, t) \\ z(0) = p \end{cases}$$

is differentiable and its derivative in p is the application mapping δp to the solution of the differential equation

$$\begin{cases} \delta z'(t) = \frac{\partial f}{\partial z}(z_p(t), p, t) \cdot \delta z(t) + \frac{\partial f}{\partial p}(z_p(t), p, t) \cdot \delta p \\ \delta z(0) = \delta p \end{cases}$$

This theorem expresses how to find properly the first order influence of a parameters change onto the state evolution. Thus, the influence of T and p onto the flame propagation evolution can be determined about the reference combustion given by $(\bar{x}, \bar{y}, \bar{p}, \bar{\theta}_{sit})$. Let us note δx and δy the sensitivity state of the differential System (11), we have

$$\begin{cases} \frac{dX}{d\tau} = A(\tau) \cdot X + B(\tau) \cdot \begin{pmatrix} \delta p \\ \delta T \end{pmatrix} \\ X(0) = \begin{pmatrix} 0 \\ C^T \end{pmatrix} \cdot \delta p \end{cases} \quad (12)$$

with

$$\begin{aligned} X &= (\delta x \ \delta y)^T \\ A(\tau) &= \begin{pmatrix} \frac{\partial F}{\partial x}(\bar{x}, \bar{y}, \bar{p}, \tau, \bar{T}) & \frac{\partial F}{\partial y}(\bar{x}, \bar{y}, \bar{p}, \tau, \bar{T}) \\ \frac{\partial G}{\partial x}(\bar{x}, \bar{y}, \bar{p}, \tau, \bar{T}) & \frac{\partial G}{\partial y}(\bar{x}, \bar{y}, \bar{p}, \tau, \bar{T}) \end{pmatrix} \\ B(\tau) &= \begin{pmatrix} \frac{\partial F}{\partial p}(\bar{x}, \bar{y}, \bar{p}, \tau, \bar{T}) & \frac{\partial F}{\partial T}(\bar{x}, \bar{y}, \bar{p}, \tau, \bar{T}) \\ \frac{\partial G}{\partial p}(\bar{x}, \bar{y}, \bar{p}, \tau, \bar{T}) & \frac{\partial G}{\partial T}(\bar{x}, \bar{y}, \bar{p}, \tau, \bar{T}) \end{pmatrix} \end{aligned} \quad (13)$$

Let Γ be the solution of the following differential equation

$$\begin{cases} \frac{d\Gamma}{d\tau} = -A(\tau)^T \cdot \Gamma \\ \Gamma(1) = \begin{pmatrix} 1 \\ 0 \end{pmatrix} \end{cases} \quad (14)$$

By the adjoint lemma (e.g. [15]), we have

$$\Gamma(1)^T X(1) - \Gamma(0)^T X(0) = \int_0^1 \Gamma(\tau)^T B(\tau) d\tau \begin{pmatrix} \delta p \\ \delta T \end{pmatrix}$$

i.e.

$$\delta x(1) - \Gamma(0)^T \begin{pmatrix} 0 \\ C^T \end{pmatrix} \delta p = \int_0^1 \Gamma(\tau)^T B(\tau) d\tau \begin{pmatrix} \delta p \\ \delta T \end{pmatrix}$$

It is desired to keep the CA_{50} to its reference value \overline{CA}_{50} . Equivalently, the terminal condition is thus $\delta x(1) = 0$. This gives the following static relation which implicitly defines the correction δT as a function of the known disturbances δp

$$-\Gamma(0)^T \cdot \begin{pmatrix} 0 \\ C^T \end{pmatrix} \delta p = \int_0^1 \Gamma(\tau)^T B(\tau) d\tau \cdot \begin{pmatrix} \delta p \\ \delta T \end{pmatrix} \quad (15)$$

where Γ is the solution of (14). This equation can be solved in terms of δT as a function of δp (see (16) and (17)).

C. Practical computation of the sit correction

Finally, the inverse variable change $\tau = \frac{\theta - \bar{\theta}_{sit}}{\bar{T}}$, $\bar{T} = \overline{CA}_{50} - \bar{\theta}_{sit}$, $\delta T = -\delta\theta_{sit}$ in equation (15) gives

$$-\Gamma_2(\bar{\theta}_{sit})^T \begin{pmatrix} 0 \\ C^T \end{pmatrix} \delta p = \int_{\bar{\theta}_{sit}}^{\overline{CA}_{50}} \Gamma_2(\theta)^T B_2(\theta) d\theta \cdot \begin{pmatrix} \delta p \\ -\delta\theta_{sit} \\ \overline{CA}_{50} - \bar{\theta}_{sit} \end{pmatrix} \quad (16)$$

with Γ_2 , and B_2 being $(\bar{\xi} \triangleq (\bar{x}, \bar{y}, \bar{p}))$

$$B_2(\theta) = \begin{pmatrix} B_2^{11}(\theta) & B_2^{12}(\theta) \\ B_2^{21}(\theta) & B_2^{22}(\theta) \end{pmatrix}$$

$$B_2^{11}(\theta) = \frac{\partial f}{\partial p}(\bar{\xi}, \theta)$$

$$B_2^{12}(\theta) = f(\bar{\xi}, \theta) + (\theta - \overline{CA}_{50}) \frac{\partial f}{\partial \theta}(\bar{\xi}, \theta)$$

$$B_2^{21}(\theta) = \frac{\partial g}{\partial p} f(\bar{\xi}, \theta)$$

$$B_2^{22}(\theta) = g(\bar{\xi}, \theta) + (\theta - \overline{CA}_{50}) \frac{\partial g}{\partial \theta}(\bar{\xi}, \theta)$$

$$A_2(\theta) = \begin{pmatrix} \frac{\partial f}{\partial x}(\bar{\xi}, \theta) & \frac{\partial g}{\partial x}(\bar{\xi}, \theta) \\ \frac{\partial f}{\partial y}(\bar{\xi}, \theta) & \frac{\partial g}{\partial y}(\bar{\xi}, \theta) \end{pmatrix}$$

In summary, the following proposition holds

Proposition 1. Equation (15) defines a first order solution to Problem 2 and Equation (16) defines a first order solution to Problem 1.

V. RESULTS

A. Controller design

Solving Equation (16) leads to the following correction

$$\delta\theta_{sit} = (\overline{CA}_{50} - \bar{\theta}_{sit}) \cdot \bar{\Lambda} \cdot \delta p \quad (17)$$

with

$$\bar{\Lambda} = \frac{\int_{\bar{\theta}_{sit}}^{\overline{CA}_{50}} \Gamma_2(\theta)^T \begin{pmatrix} B_2^{11}(\theta) \\ B_2^{21}(\theta) \end{pmatrix} d\theta + \Gamma_2(\bar{\theta}_{sit})^T \begin{pmatrix} 0 \\ C^T \end{pmatrix}}{\int_{\bar{\theta}_{sit}}^{\overline{CA}_{50}} \Gamma_2(\theta)^T \begin{pmatrix} B_2^{12}(\theta) \\ B_2^{22}(\theta) \end{pmatrix} d\theta}$$

In practice, the correction $\delta\theta_{sit}$ is easily computable since $\bar{\Lambda}$ depends only on known parameters of the current working point (N_e, m_{air}) and on the model equations. Then the *sit* correction can be directly added to the nominal spark timing found in static look-up tables. Again, the proposed strategy does not need any in-cylinder sensor feedback, i.e. *no in-cylinder pressure sensors are required*.

B. Results with the Amesim Simulation software

1) *Simulation setup*: The strategy presented in Section V-A has been validated on the simulation software AMESim [16]. The combustion model used in the simulator is presented in [10], and has been validated in [17] for engine control purposes. Basically, this simulation model is almost the same as the one presented in Section II. In fact, wall heating losses are now taken into account and the flame geometrical shape is slightly different (see Section II-C.1).

2) *Simulation Results*: Figure 4 reports simulation results. We simulate transient operation by creating arbitrary offsets on the following parameters: in-cylinder pressure at *ivc* P_{ivc} , burned gases mass m_{bg} , and intake valve closing crankshaft angle θ_{ivc} (the in-cylinder temperature offset at the *ivc* is then computed according to the perfect gases relation $P_{ivc} V(\theta_{ivc}) = (m_{air} + m_{bg}) r T_{ivc}$. These offsets are presented in Figure 4c. Both state x and y histories are represented in Figures 4a and 4b for different working conditions.

- The black curve represents the reference combustion. It has been obtained for a reference spark timing $\bar{\theta}_{sit}$ and thus defines the reference \overline{CA}_{50} (about 369 deg on the considered point).
- The red dotted curves correspond to the combustions resulting from the introduction of the previously discussed offsets. In this case, no *sit* correction is used. One can see in Figure 4a that the CA_{50} significantly drifts away from its reference value.
- The blue curves correspond to the same combustions in which we have activated the proposed *sit* correction (see 17). Thus, the spark timing is different for each combustion (see “o” markers in Figures 4a and 4b). The resulting CA_{50} can be seen in Figure 4a. The error between the actual and the reference CA_{50} has been drastically reduced.

We thus validate the proposed approach at the light of the presented results. The *sit* correction permits to reduce the CA_{50} offset in the presence of arbitrary airpath offsets. Residual CA_{50} errors are due to: 1) the differences between the control model used to compute the correction and the simulation model used to test the correction; 2) the first order approximation used to compute the correction. Further it is expected that the reduction of the CA_{50} error will improve the torque trajectory tracking and the overall driveability.

VI. CONCLUSION AND FUTURE DIRECTION

In this preliminary work, we have proven that a phenomenological model can be used to compute open-loop spark timing correction to control the CA_{50} . Simulation

validation of this correction has been carried out on the AMESim platform. Results show that the proposed method effectively permits to control in open-loop the CA_{50} closer to its reference value. The method is very general and can be applied to any improved phenomenological model. Its main advantage is that *it does not require any in-cylinder sensor*.

The next step is to validate this correction on experimental test-benches. Based on the simulation results, one can reasonably expect improvements in experimental transient operations.

VII. ACKNOWLEDGEMENT

The authors would like to gratefully thank Gilles Corde for his scientific support.

REFERENCES

- [1] H. Kleeberg, D. Tomazic, O. Lang, and K. Habermann, "Future potential and development methods for high output turbocharged direct-injected gasoline engines," in *Proc. SAE World Congress*, no. 2006-01-0046, 2006.
- [2] T. Leone, E. Christenson, and R. Stein, "Comparison of variable camshaft timing strategies at part load," in *Proc. of SAE Conference*, no. 960584, 1996.
- [3] T. Leroy, J. Chauvin, N. Petit, and G. Corde, "Motion planning control of the airpath of a S.I. engine with valve timing actuators," in *International federation of automatic control*, 2007.
- [4] A. Stefanopoulou and I. Kolmanovsky, "Dynamic scheduling of internal exhaust gas recirculation systems," in *Proc. IMECE*, vol. 61, 1997, pp. 671–678.
- [5] M. Jankovic, F. Frischmuth, A. Stefanopoulou, and J. Cook, "Torque management of engines with variable cam timing," in *Control Systems Magazine, IEEE*, vol. 18, 1998, pp. 34–42.
- [6] T.-C. Tseng and W. Cheng, "An adaptive air/fuel ratio controller for SI engine throttle transients," in *Proc. of SAE Conference*, no. 1999-01-0552, 1999.
- [7] L. Guzzella, M. Simons, and H. Geering, "Feedback linearizing air/fuel-ratio controller," in *Control Eng. Practice*, vol. 5, no. 8, 1997, pp. 1101–1105.
- [8] J. Heywood, *Internal combustion engine fundamental*. Mc Graw-Hill, Inc, 1988.
- [9] L. Eriksson, L. Nielsen, and M. Glavenius, "Closed loop ignition control by ionization current interpretation," in *SAE journal of engines*, vol. 106, 1997, pp. 1216–1223.
- [10] F.-A. Lafossas, O. Colin, F. L. Berr, and P. Menegazzi, "Application of a new 1d combustion model to gasoline transient engine operation," in *Proc. SAE World Congress*, no. 2005-01-2107, 2005.
- [11] M. Metghalchi and J. Keck, "Burning velocities of mixture of air with methanol iso-octane and indolene at high pressure and temperature," in *Combust. Flame*, vol. 48, 1982, pp. 191–210.
- [12] T. Leroy, G. Alix, A. Duparchy, and F. Le Berr, "Modelling fresh air charge and residual gas fraction on a dual independent variable valve timing SI engine," in *Proc. SAE World Congress*, no. 2008-01-0983, 2008.
- [13] P. Andersson, "Air charge estimation in turbocharged spark ignition engines," Ph.D. dissertation, Linköpings Universitet, dec 2005.
- [14] J. Hale, *Ordinary Differential Equation*, 2nd ed. Krieger Publish Compagny, 1980.
- [15] T. Kailath, *Linear systems*. Prentice-Hall, Inc., 1980.
- [16] LMS IMAGINE. [Online]. Available: <http://www.lmsintl.com/imagen>
- [17] F. Le Berr, M. Miche, G. Le Sollic, F.-A. Lafossas, and G. Colin, "Modelling of a turbocharged SI engine with variable camshaft timing for engine control purposes," in *Proc. of SAE Conference*, no. 2006-01-3264, 2006.

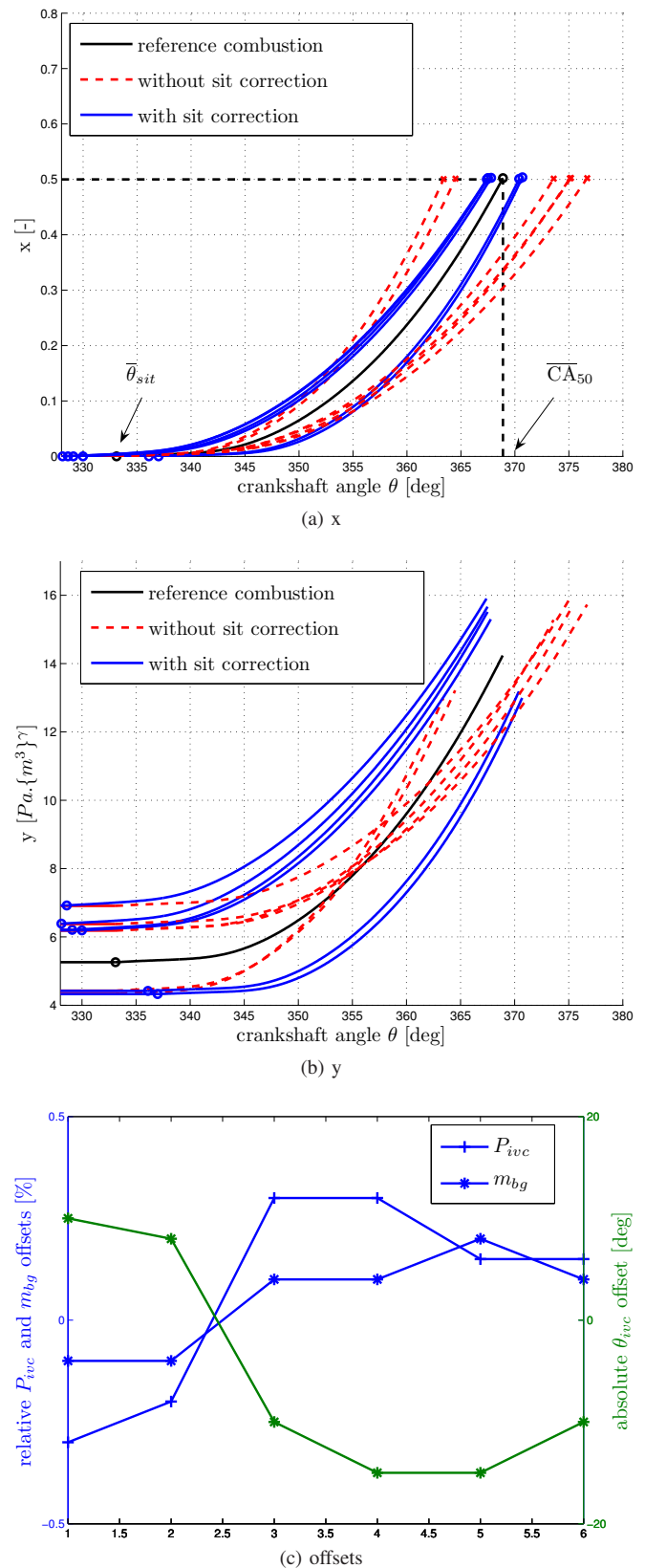


Fig. 4. Simulation results: mass fraction of burned fuel (state x in the model) and Pv^γ (state y in the model) for different offsets of thermodynamic and physical parameters at ivc . Black curve: reference combustion, red dotted curves: combustion with parameters offsets without *sit* correction, blue curves: combustion with the same parameters offsets and with *sit* correction. In (a) and (b), "o" marks the spark initiation.